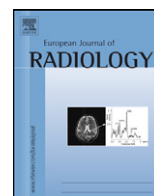




Contents lists available at ScienceDirect

European Journal of Radiology

journal homepage: www.elsevier.com/locate/ejrad



Effective dose range for dental cone beam computed tomography scanners

Ruben Pauwels^{a,*}, Jilke Beinsberger^{a,1}, Bruno Collaert^{b,2}, Chrysoula Theodorakou^{c,d,3},
Jessica Rogers^{e,3}, Anne Walker^{c,3}, Lesley Cockmartin^{f,4}, Hilde Bosmans^{f,5}, Reinhilde Jacobs^{a,6},
Ria Bogaerts^{g,7}, Keith Horner^{d,8}, The SEDENTEXCT Project Consortium⁹

^a Oral Imaging Center, School of Dentistry, Oral Pathology and Maxillofacial Surgery, Faculty of Medicine, Catholic University of Leuven, Belgium

^b Center for Periodontology and Implantology, Heverlee, Belgium

^c North Western Medical Physics, The Christie NHS Foundation Trust, Manchester Academic Health Sciences Centre, UK

^d School of Dentistry, University of Manchester, Manchester Academic Health Sciences Centre, UK

^e School of Medicine, University of Manchester, Manchester Academic Health Sciences Centre, UK

^f Department of Radiology, University Hospital Gasthuisberg, Leuven, Belgium

^g Department of Experimental Radiotherapy, University Hospital Gasthuisberg, Katholieke Universiteit Leuven, Belgium

ARTICLE INFO

Article history:

Received 26 August 2010

Received in revised form

10 November 2010

Accepted 12 November 2010

Keywords:

Cone beam computed tomography

Dentomaxillofacial

Effective radiation dose

Thermoluminescent dosimetry

ABSTRACT

Objective: To estimate the absorbed organ dose and effective dose for a wide range of cone beam computed tomography scanners, using different exposure protocols and geometries.

Materials and methods: Two Alderson Radiation Therapy anthropomorphic phantoms were loaded with LiF detectors (TLD-100 and TLD-100H) which were evenly distributed throughout the head and neck, covering all radiosensitive organs. Measurements were performed on 14 CBCT devices: 3D Accuitomo 170, Galileos Comfort, i-CAT Next Generation, Iluma Elite, Kodak 9000 3D, Kodak 9500, NewTom VG, NewTom VGi, Pax-Uni3D, Picasso Trio, ProMax 3D, Scanora 3D, SkyView, Veraviewepocs 3D. Effective dose was calculated using the ICRP 103 (2007) tissue weighting factors.

Results: Effective dose ranged between 19 and 368 μ Sv. The largest contributions to the effective dose were from the remainder tissues (37%), salivary glands (24%), and thyroid gland (21%). For all organs, there was a wide range of measured values apparent, due to differences in exposure factors, diameter and height of the primary beam, and positioning of the beam relative to the radiosensitive organs.

Conclusions: The effective dose for different CBCT devices showed a 20-fold range. The results show that a distinction is needed between small-, medium-, and large-field CBCT scanners and protocols, as they are applied to different indication groups, the dose received being strongly related to field size. Furthermore, the dose should always be considered relative to technical and diagnostic image quality, seeing that image quality requirements also differ for patient groups. The results from the current study indicate that the optimisation of dose should be performed by an appropriate selection of exposure parameters and field size, depending on the diagnostic requirements.

© 2010 Elsevier Ireland Ltd. All rights reserved.

1. Introduction

In recent years, cone beam computed tomography (CBCT) has become a widely accepted radiographic tool for diagnosis, treatment planning and follow-up in dentistry. This modality is also known as digital volume tomography (DVT). CBCT allows the acquisition of three-dimensional volumes of the dental arches and surrounding tissues at a high spatial resolution and a low radiation dose. There are a number of different dental applications that benefit from the use of CBCT, each with specific requirements regarding the size of the acquired volume and the image quality in terms of spatial and contrast resolution [1].

* Corresponding author at: Oral Imaging Center, Faculty of Medicine, Katholieke Universiteit Leuven, Kapucijnenvoer 7, 3000 Leuven, Belgium. Tel.: +32 16 33 29 51.

E-mail addresses: ruben.pauwels@med.kuleuven.be, pauwelsruben@hotmail.com (R. Pauwels), jilke.beinsberger@student.kuleuven.be (J. Beinsberger), collaert@paro-implanto.be (B. Collaert), Christie.Theodorakou@physics.cr.man.ac.uk (C. Theodorakou), jessica.rogers12@yahoo.co.uk (J. Rogers), Anne.Walker@physics.cr.man.ac.uk (A. Walker), lesley.cockmartin@med.kuleuven.be (L. Cockmartin), hilde.bosmans@uz.kuleuven.ac.be (H. Bosmans), reinhilde.jacobs@med.kuleuven.be (R. Jacobs), Ria.Bogaerts@med.kuleuven.be (R. Bogaerts), keith.horner@manchester.ac.uk (K. Horner).

¹ Tel.: +32 16 33 29 51.

² Tel.: +32 16 22 29 90.

³ Tel.: +44 161 446 3539.

⁴ Tel.: +32 16 343616.

⁵ Tel.: +32 16 347750; fax: +32 16 343765.

⁶ Tel.: +32 16 332410; fax: +32 16 332951.

⁷ Tel.: +32 16 343637; fax: +32 16 347610.

⁸ Tel.: +44 161 275 6726; fax: +44 161 275.

⁹ Listing of partners on www.sedentext.eu.

Table 1
Technical parameters of CBCT devices.

CBCT	Manufacturer	Protocol	FOV (cm)	Voltage (kV)	mAs
3D Accuitomo 170	J. Morita, Kyoto, Japan	Maxilla	10 × 5	90	87.5
		Lower jaw molar region	4 × 4	90	87.5
Galileos Comfort	Sirona Dental Systems, Bensheim, Germany	Maxillofacial	15 × 15	85	28
		i-CAT Next Generation	Maxillofacial	16 × 13	120
Iluma Elite	Imtec (3M), Ardmore, OK, USA	Mandible	16 × 6	120	18.5
		Kodak 9000 3D	Maxillofacial	21 × 14	120
Kodak 9500	Kodak Dental Systems, Carestream Health, Rochester, NY, USA	Upper jaw front region	5 × 3.7	70	107
		Lower jaw molar region	5 × 3.7	70	107
NewTom VG	Quantitative Radiology, Verona, Italy	Maxillofacial	20 × 18	90	108
		NewTom VGi	Dentoalveolar	15 × 8	90
PaX-Uni3D	VATECH, Yongin, Republic of Korea	Maxillofacial	23 × 23	110	10.4
		Picasso Trio	Maxillofacial	15 × 15	110
Promax3D	Planmeca Oy, Helsinki, Finland	Dentoalveolar	12 × 8	110	43
		Scanora 3D	Upper jaw front region	5 × 5	85
SkyView	MyRay, Cefla Dental Group, Imola, Italy		Dentoalveolar - standard dose	12 × 7	85
		Dentoalveolar - low dose	12 × 7	85	91
Veraviewepocs 3D	J. Morita, Kyoto, Japan	Dentoalveolar - standard dose	8 × 8	84	169
		Dentoalveolar - low dose	8 × 8	84	19.9
Veraviewepocs 3D	J. Morita, Kyoto, Japan	Dentoalveolar	10 × 7.5	85	30
		Mandible	10 × 7.5	85	30
Veraviewepocs 3D	J. Morita, Kyoto, Japan	Maxilla	10 × 7.5	85	30
		Maxillofacial	14.5 × 13.5	85	48
Veraviewepocs 3D	J. Morita, Kyoto, Japan	Maxillofacial	17 × 17	90	51.5
		Dentoalveolar	8 × 8	70	51

The number of CBCT devices available on the market has increased substantially and new models are being developed and released on a continuous basis. These devices exhibit a wide variability in terms of crucial exposure parameters such as the X-ray spectrum (voltage peak and filtration), X-ray exposure (mA and number of projections) and volume of the exposed field. Also, many devices allow a degree of versatility regarding the exposure, allowing the operator to select certain exposure parameters. It is clear that the range of devices and imaging protocols that are available will result in different absorbed radiation doses for the patient with, to some extent, the amount of dose being reflected in the image quality of the scan. Radiation dose and image quality, together with the size of the field of view (FOV), determine whether or not a certain CBCT imaging protocol from a given device is suitable for a specific dental application by following the generally applied ALARA (As Low As Reasonably Achievable) principle of radiation exposure [2,3].

To measure the radiation risk for patients from a radiographic modality, the effective dose is still accepted as the most suitable figure of merit, even though alternatives are under consideration [4–7]. The effective dose is measured in practice using an anthropomorphic phantom, representing the shape and attenuation of an average human, most commonly an adult male [8]. There have been a number of studies measuring the effective dose on dental CBCT using thermoluminescent dosimeters (TLDs) in combination with a human phantom [9–19]. These studies provide some estimation of the range of doses that are obtained from these devices, but are not comparable, seeing that different types of phantoms are used as well as different TLD positioning schemes, with the number of TLDs applied to the different organs often being too low for an accurate and reproducible estimation of the organ and effective doses [11–18].

The aim of the current study was to perform a broad evaluation of the organ and effective doses obtained from CBCT, using a wide range of devices and imaging protocols.

2. Materials and methods

To estimate the effective dose for an average adult male, two similar types of anthropomorphic male Alderson Radiation Therapy (ART) phantoms (Radiology Support Devices Inc., CA, USA) were

used. They represent an average man (175 cm tall, 73.5 kg) and consist of a polymer mould simulating the bone, embedded in soft tissue equivalent material. They are transected into 2.5 cm thick slices, each containing a grid for TLD placement. The upper 11 slices (*i.e.* head and neck region) were used for TLD measurements, seeing that there is no significant dose found in the lower parts for dental examinations [19].

The phantoms were scanned on a variety of available CBCT devices, combining different exposure protocols when possible. The phantoms were positioned as closely as possible to a typical patient with the help of local radiographic staff using the positioning aids provided for the scanner. The following CBCT devices were included: 3D Accuitomo 170, Galileos Comfort, i-CAT Next Generation, Iluma Elite, Kodak 9000 3D, Kodak 9500, NewTom VG, NewTom VGi, Pax-Uni3D, Picasso Trio, ProMax 3D, Scanora 3D, SkyView, Veraviewepocs 3D. Device parameters for different protocols that were included are given in Table 1.

Two types of TLDs were used for the measurements: TLD-100 (LiF:Mg,Ti) and TLD-100H (LiF: Mg,Cu,P). Calibration of the TLD-100H was performed free in air against an ionisation chamber with calibration traceable to national standards (National Physical Laboratory, London, UK), using a conventional diagnostic X-ray tube at 80 kV. The chips were read using a Harshaw 5500 automatic TLD reader. Calibration of the TLD-100 was performed by irradiating internal calibration dosimeters for each experiment using a ⁹⁰Sr source. The source itself was calibrated using an ionisation chamber with a calibration factor traceable to a Secondary Standard Dosimetry Laboratory (SSDL, Gent, Belgium). The read-out of the TLDs was performed by a Harshaw 6600 reader.

For each slice, placement of the TLDs was carefully considered with input from dental radiologists to ensure that there was an even spread over the different radiosensitive organs. Due to small differences between the two phantoms, TLD positioning was determined for each phantom separately. In total, 147 TLDs were used for one phantom and 152 for the other. Background dose was measured using non-irradiated TLDs and subtracted from all field TLD values.

Two intercomparisons were performed to ensure that the variability between measurements performed on the two phantoms using different TLD types and positioning was within an acceptable range. Differences between TLD types were investigated, and identical exposures were applied to the two phantoms using one

Table 2
 ICRP 103 (2007) Tissue weighting factors.

Organ	Weighting factor
Gonads	0.08
Red bone marrow ^a	0.12
Colon	0.12
Lung	0.12
Stomach	0.12
Bladder	0.04
Breast	0.12
Liver	0.04
Oesophagus	0.04
Thyroid ^a	0.04
Skin ^a	0.01
Bone surface ^a	0.01
Brain ^a	0.01
Salivary glands ^a	0.01
Remainder ^{a,b}	0.12

^a Head and neck or whole body organ, included in current study.

^b Adipose tissue, adrenals, extrathoracic (ET) region, gall bladder, heart, kidneys, lymphatic nodes, muscle, oral mucosa, pancreas, prostate, small intestine, spleen, thymus, uterus/cervix.

TLD type. Based on the results of the intercomparison, it was not deemed necessary to apply a correction factor.

The following calculation was used to determine the equivalent dose or radiation weighted dose H_T for all organs or tissues T:

$$H_T = w_R \sum_i f_i D_{Ti}$$

In this formula, w_R is the radiation weighting factor (being 1 for X-rays), f_i the fraction of tissue T in slice i , and D_{Ti} the average absorbed dose of tissue T in slice i , the summation being over all slices. For the brain, salivary glands, thyroid gland, oral mucosa and extrathoracic airways, calculation of H_T was straightforward since these organs are found completely within the head and neck. For bone and skin, the organ fractions reported by Huda et al. [8] were used. For muscle and lymph nodes, it was estimated that 5% of these organs are found within the head and neck, and an overall fraction of 0.05 was applied [16].

In order to calculate the contribution E_T of each organ to the effective dose, the organ radiation weighted dose is multiplied by the tissue weighting factor w_T , which expresses the contribution of this tissue to the overall radiation detriment from stochastic effects:

$$E_T = w_T H_T$$

The tissue weighting factors that are defined in the latest recommendations of the International Commission on Radiological Protection were applied (Table 2) [4]. The effective dose is calculated by taking the sum of the contribution E_T for all relevant organs as shown in Table 2. The oesophagus was originally included in the calculation, but it was found that this organ does not provide a significant contribution to the effective dose.

As an additional evaluation, organ doses for red bone marrow, thyroid, salivary glands and remainder organs were recalculated

using a limited number of selected TLDs, hereby mimicking the positioning protocol used by Ludlow et al. [12] which has been adapted by other authors [11,16,18]. Using this protocol, 24 TLDs are used for effective dose calculation. The average and maximum variability between organ dose estimations using the two methods was calculated.

3. Results

Due to the large differences in acquired volume, which is one of the main determinants of the effective dose, the results were split up by dividing the CBCT devices into three categories: large FOV (maxillofacial), medium FOV (dentoalveolar) and small FOV (localised). This allows for a fairer comparison between protocols, as different FOV sizes are used for different subsets of patients. It should be noted that some devices allow for a range of field sizes, and can therefore be found in more than one category, thereby widening their application range.

Table 3 gives the absorbed organ doses and effective dose for large FOV protocols. The effective dose ranged between 68 and 368 μ Sv. The highest absorbed dose was in the salivary glands, although the largest contribution to the effective dose was provided by the remainder tissue due to its higher weighting factor.

Dose measurements from medium FOV protocols are shown in Table 4, showing effective doses between 28 and 265 μ Sv. Compared with the results from the large field protocols, organ doses were distributed similarly, although it is seen that the contribution of the brain was lower.

Table 5 shows the results for the small FOV protocols. The effective dose ranged between 19 and 44 μ Sv. From these results, the effect of FOV positioning can be observed. Comparing an upper jaw, frontal region with a lower jaw, molar region scan from the Kodak 9000 3D, it is seen that there were large differences regarding the absorbed dose for the salivary glands, thyroid gland, oral mucosa and extrathoracic airways.

The average doses for all devices for each FOV group are shown in Fig. 1. The average doses for large, medium and small FOVs were 131, 88 and 34 μ Sv respectively. The standard deviations were 91 (70% of mean), 70 (83%) and 14 (37%), showing large variability of doses for large and medium FOV groups.

Fig. 2 illustrates the average contribution of each of the measured organs to the effective dose. The remainder organs have the highest contribution, followed by the salivary glands and thyroid gland. Contributions of brain, bone surface and skin are almost negligible. No notable differences were seen when comparing the contributions for small, medium and large FOVs separately.

Variability between organ doses estimations using the current TLD positioning, and recalculations using the positioning protocol devised by Ludlow et al. [16] are shown in Table 6. The largest deviations were seen for small FOV protocols, showing particularly high deviations for the thyroid gland and remainder tissues. As seen in Fig. 2, the four organs that were selected for dose recalculation comprise 95% of the effective dose.

Table 3
 Absorbed organ dose and effective dose for large FOV (maxillofacial) protocols.

	Galileos Comfort	i-CAT N.G.	Iluma Elite	Kodak 9500	NewTom VG	NewTom VGi	Scanora 3D	SkyView
RBM	82	116	660	206	115	186	86	134
Thyroid	380	355	1230	585	354	2045	296	474
Skin	55	54	277	92	50	98	55	58
Bone surface	83	124	667	215	163	184	94	125
Salivary glands	2104	1830	7225	2676	1690	2855	1568	1582
Brain	124	375	3415	1205	251	605	255	719
Remainder	292	260	1034	380	281	436	221	224
Effective dose	84	83	368	136	83	194	68	87

Table 4
Absorbed organ dose and effective dose for medium FOV (dentoalveolar or single jaw) protocols.

	3D Accuitomo 170	i-CAT N.G.	Kodak 9500	NewTom VGi	Picasso Trio	Picasso Trio	ProMax 3D	ProMax 3D	Scanora 3D	Scanora 3D	Scanora 3D	Veraviewepocs 3D
Protocol ^a	Upper jaw				High dose	Low dose	High dose	Low dose	Upper jaw	Lower jaw	Both jaws	
Red bone marrow	112	33	85	294	126	62	88	27	42	34	37	55
Thyroid	148	251	541	1293	551	583	1021	202	148	352	240	330
Skin	62	25	51	145	113	56	145	15	30	29	31	69
Bone surface	112	33	84	299	156	57	121	26	50	35	39	57
Salivary glands	2138	973	2166	6372	2982	1837	2576	596	1285	1052	1117	1956
Brain	189	46	91	431	134	39	53	28	45	25	31	40
Remainder	85	172	304	881	432	254	346	83	178	147	155	267
Effective dose	54	45	92	265	123	81	122	28	46	47	45	73

^a If not specified, the positioning of the FOV is dentoalveolar (both jaws).

Table 5
Absorbed organ dose and effective dose for small FOV (localised) protocols.

	3D Accuitomo 170	Kodak 9000 3D	Kodak 9000 3D	Pax-Uni3D
FOV positioning	Lower jaw, molar region	Upper jaw, front region	Lower jaw, molar region	Upper jaw, front region
Red bone marrow	37	21	78	47
Thyroid	195	30	251	209
Skin	32	25	24	55
Bone surface	37	27	35	49
Salivary glands	2120	523	709	1073
Brain	37	18	290	28
Remainder	70	74	86	146
Effective dose	43	19	40	44

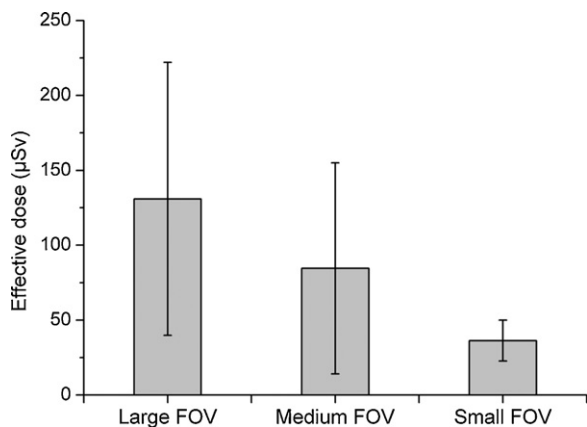


Fig. 1. Average effective dose for CBCT devices, divided into groups based on field of view size. Standard deviations are shown for each group.

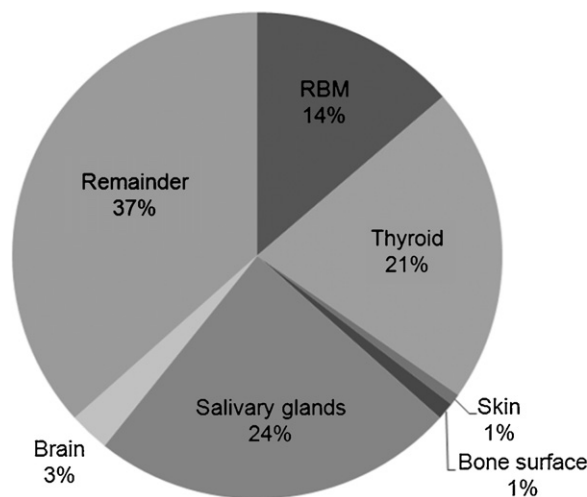


Fig. 2. Average contribution of organs to effective dose.

4. Discussion

In the present study, effective dose estimations were performed on a wide range of dental CBCT devices, investigating the difference in dose due to variability in FOV size, tube output and exposure factors.

A large number of TLDs was used to ensure that the measurement was as accurate as possible. The TLDs were positioned throughout the head and neck to correctly cover all radiosensitive organs. By performing measurements on a large number of CBCT devices, differences in dose between the different CBCTs could reliably be determined. Comparing these results with previous studies should be done with caution, as previous studies have used other phantoms and different numbers and positioning of TLDs, often using too few TLDs for an accurate measurement [11–18,20–21]. It must be stressed that for this type of dose measurement, the only way to estimate precisely the absorbed dose for any organ is to use TLDs at as many locations as possible for this organ, because the absorbed dose is an average dose. This is of particular concern in dental CBCT; due to the large range of FOV sizes and the different possible positioning of this FOV within the dentomaxillofacial region, the position of the primary beam is variable, and each single location in the vicinity of the scanned region can show large variability depending on its relative position to the isocentre. This is shown by the different protocols for the Scanora 3D; by changing the position of the FOV a few cm to move from a lower jaw to a dentoalveolar or an upper jaw examination, large differences are seen for individual TLD values. However, these single TLDs have limited effect on the effective dose, seeing that only the thyroid dose changes significantly. Using a limited number of TLDs may

Table 6
Variability of organ dose calculations using a low number of TLDs.

Organ	Average deviation (%)	Maximum deviation (%)
Red bone marrow	21	40
Thyroid	18	26
Salivary glands	28	76
Remainder	25	80

underestimate or overestimate this kind of change in positioning. By recalculating the organ doses presented in this study, it was seen that organ dose estimations using a low number of TLDs can deviate 18–28% with differences up to 80%. These values indicate that a large number of TLDs is needed for accurate effective dose estimation, in particular for red bone marrow, thyroid, salivary glands and remainder tissues.

From the results, it is seen that a single average effective dose is not a concept that should be used for the modality of CBCT as a whole, when comparing to alternative radiographic methods such as panoramic, intra-oral radiography and multislice CT (MSCT). The range of doses between the devices is too large to consider them as a single modality; even though the geometry of the image acquisition is basically the same, the differences in collimation of the cone beam, as well as the X-ray exposure factors, lead to considerable differences in absorbed dose for all organs in the head and neck region. However, a general conclusion based on the presented values is that the effective dose from most devices is found in the 20–100 μ Sv range, being higher than doses for 2D radiographic methods used in dentistry but well below reported doses for common MSCT protocols [9–12,19–22]. Some devices show an elevated dose due to relatively high kV and mAs settings combined with a large FOV, attaining a dose range comparable with low-dose MSCT protocols [19].

The results should be interpreted carefully, due to the interplay between image quality, size of the scanned volume and absorbed radiation dose to different tissues. Therefore, the main goal of the study was not to compare the performance of different CBCT devices, as this cannot be done based on dosimetric results alone. Different studies have already pointed out that CBCT devices can have different application ranges, based on their maximum FOV size, collimation options, and diagnostic image quality [1,3,9,12,17]. Therefore, the radiation dose from these devices can be seen as a function of the diagnostic application. From that perspective, a key paradigm for dose optimisation is to ensure that patient scans are made using an exposure protocol which leads to an acceptable image for their specific indication [2,3]. The two key factors for an acceptable image are an appropriate size and positioning of the FOV and an acceptable quality of the reconstructed image. The only distinction made between the devices within this study was based on the size of the FOV, as this is a main determinant of possible diagnostic applications. Further study is required to bring the image quality into play, on a technical and diagnostic level. By investigating technical image quality, the relation between the exposure from CBCT devices and the image quality performance in terms of noise, sharpness, contrast and artefacts, can be quantified; diagnostic quality studies would link all quantifications of dose of image quality to performance evaluation on a clinical level.

Acknowledgements

The research leading to these results has received funding from the European Atomic Energy Community's Seventh Framework

programme FP7/2007–2011 under grant agreement no. 212246 (SEDETEXCT: Safety and Efficacy of a New and Emerging Dental X-ray Modality).

The Manchester authors acknowledge the support of the NIHR Manchester Biomedical Research Centre.

References

- [1] Scarfe WC, Farman AG, Sukovic P. Clinical applications of cone-beam computed tomography in dental practice. *J Can Dent Assoc* 2006;72(1):75–85.
- [2] Martin CJ, Sutton DG, Sharp PF. Balancing patient dose and image quality. *Appl Radiat Isot* 1999;50(1):1–19.
- [3] Farman AG. ALARA still applies. *Oral Surg Oral Med Oral Pathol Oral Radiol Endod* 2005;100(4):395–7.
- [4] International Commission on Radiological Protection. Recommendations of the International Commission on Radiological Protection. ICRP Publication 103. Ann ICRP 37. Oxford, UK: Pergamon Press, 2007.
- [5] Martin CJ. Effective dose: how should it be applied to medical exposures? *Br J Radiol* 2007;80(956):639–47.
- [6] Brenner DJ. Effective dose: a flawed concept that could and should be replaced. *Br J Radiol* 2008;81(967):521–3.
- [7] Thilander-Klang A, Helmrot E. Methods of determining the effective dose in dental radiology. *Radiat Prot Dosimetry* 2010;139(1–3):306–9.
- [8] Huda W, Sandison GA. Estimation of mean organ doses in diagnostic radiology from Rando phantom measurements. *Health Phys* 1984;47(3):463–7.
- [9] Loubele M, Bogaerts R, Van Dijck E, et al. Comparison between effective radiation dose of CBCT and MSCT scanners for dentomaxillofacial applications. *Eur J Radiol* 2009;71(3):461–8.
- [10] Okano T, Harata Y, Sugihara Y, et al. Absorbed and effective doses from cone beam volumetric imaging for implant planning. *Dentomaxillofac Radiol* 2009;38(2):79–85.
- [11] Suomalainen A, Kiljunen T, Käser Y, Peltola J, Kortensniemi M. Dosimetry and image quality of four dental cone beam computed tomography scanners compared with multislice computed tomography scanners. *Dentomaxillofac Radiol* 2009;38(6):367–78.
- [12] Ludlow JB, Ivanovic M. Comparative dosimetry of dental CBCT devices and 64-slice CT for oral and maxillofacial radiology. *Oral Surg Oral Med Oral Pathol Oral Radiol Endod* 2008;106(1):106–14.
- [13] Silva MA, Wolf U, Heinicke F, Bumann A, Visser H, Hirsch E. Cone-beam computed tomography for routine orthodontic treatment planning: a radiation dose evaluation. *Am J Orthod Dentofacial Orthop* 2008;133(5):640.e1–5.
- [14] Ludlow JB, Davies-Ludlow LE, Brooks SL, Howerton WB. Dosimetry of 3 CBCT devices for oral and maxillofacial radiology: CB Mercuray NewTom 3G and i-CAT. *Dentomaxillofac Radiol* 2006;35(4):219–26.
- [15] Tsiklakis K, Donta C, Gavala S, Karayianni K, Kamenopoulou V, Hourdakis CJ. Dose reduction in maxillofacial imaging using low dose Cone Beam CT. *Eur J Radiol* 2005;56(3):413–7.
- [16] Roberts JA, Drage NA, Davies J, Thomas DW. Effective dose from cone beam CT examinations in dentistry. *Br J Radiol* 2009;82(973):35–40.
- [17] Hirsch E, Wolf U, Heinicke F, Silva MA. Dosimetry of the cone beam computed tomography Veraviewepocs 3D compared with the 3D Accuitomo in different fields of view. *Dentomaxillofac Radiol* 2008;37(5):268–73.
- [18] Mah JK, Danforth RA, Bumann A, Hatcher D. Radiation absorbed in maxillofacial imaging with a new dental computed tomography device. *Oral Surg Oral Med Oral Pathol Oral Radiol Endod* 2003;96(4):508–13.
- [19] Loubele M, Jacobs R, Maes F, et al. Radiation dose vs. image quality for low-dose CT protocols of the head for maxillofacial surgery and oral implant planning. *Radiat Prot Dosimetry* 2006;117(1–3):211–6.
- [20] Ngan DC, Kharbanda OP, Geenty JP, Darendeliler MA. Comparison of radiation levels from computed tomography and conventional dental radiographs. *Aust Orthod J* 2003;19(2):67–75.
- [21] Ludlow JB, Davies-Ludlow LE, White SC. Patient risk related to common dental radiographic examinations: the impact of 2007 International Commission on Radiological Protection recommendations regarding dose calculation. *J Am Dent Assoc* 2008;139(9):1237–43.
- [22] Gijbels F, Jacobs R, Bogaerts R, Debaveye D, Verlinden S, Sanderink G. Dosimetry of digital panoramic imaging Part I: patient exposure. *Dentomaxillofac Radiol* 2005;34(3):145–9.